

## Critical Behavior in Percolation Processes\*

W. G. Rudd and H. L. Frisch

*Department of Chemistry, State University of New York at Albany, Albany, New York 12203*

(Received 3 November 1969)

The Monte Carlo percolation-probability data of Frisch *et al.* are analyzed under the assumption that  $R(p)$ , the probability that a given site (bond) belongs to an infinite cluster as a function of the probability  $p$  of site (bond) occupation, has the asymptotic behavior  $R(p) \sim (p - p_c)^\beta$ , as  $p \rightarrow p_c^+$ , where  $p_c$  is the critical percolation probability. The estimated values of  $\beta$  for various lattices are tabulated.

Recent interest in critical behavior in systems such as the Ising and Heisenberg models has led us to an investigation of possible analogous behavior in percolation processes. The appearance of infinitely large clusters when the probability  $p$  of site or bond occupation is greater than a certain "critical" value is reminiscent of the onset of spontaneous magnetization in the ferromagnetic Ising problem when the temperature drops below the Curie temperature. One might therefore expect the occurrence of infinite-sized clusters to be characterized by a critical exponent  $\beta$  when  $p$  is close to the critical percolation probability  $p_c$ . The following describes an attempt to determine values of  $\beta$  for various lattices from the corresponding Monte Carlo data of Frisch *et al.*<sup>1-3</sup>

The percolation problem<sup>4</sup> can be described as follows<sup>5</sup>: Given is a regular infinite  $d$ -dimensional lattice of sites with a probability  $p$  that a given site is "occupied." Two occupied sites are said to be connected if there is a path composed only of nearest-neighbor bonds from one site to the other, such that the path crosses only occupied sites. A cluster is a set of sites which are connected to each other. A similar set of definitions applies to the problem in which bonds, rather than sites can be occupied; we will refer to these problems as bond problems, the former as site problems. We define the function  $R(p)$ , which is the probability that a given site (bond) belongs to a cluster containing an infinite number of occupied sites (bonds). Then the critical probability is defined as the minimum probability above which  $R(p)$  is non-zero:

$$\begin{aligned} R(p) &= 0 & \text{if } p < p_c \\ &> 0 & \text{if } p \geq p_c \end{aligned} \quad (1)$$

Now one can show, by combining the generating-function techniques of Fisher and Essam<sup>6</sup> with the graph-theoretical arguments of Kasteleyn and Fortuin<sup>7</sup> and of Griffiths,<sup>8</sup> that  $R(p)$  in the percolation problem is the thermodynamic analog of the zero-field spontaneous magnetization in the ferromagnetic Ising model. Hence, we expect that

$$R(p) \sim (p - p_c)^\beta, \quad (2)$$

as  $p \rightarrow p_c$  from above. Since the authors know of no reason to suspect that  $\beta$  will have the same values as those from the Ising problem, we have used the procedures outlined below to find numerical values of the critical exponent  $\beta$  from the Monte Carlo (MC) data.

Upon examining the algorithm used in the MC calculations,<sup>9</sup> one observes that the function  $P(p)$  calculated therein is actually an upper bound for the function  $R(p)$  of interest here. Thus, the critical percolation probabilities predicted by the MC calculations are systematically lower<sup>10</sup> than those values obtained from exact calculations<sup>11</sup> and series methods.<sup>12</sup> This situation leaves some latitude in how to go about doing the curve fitting.

The most obvious approach is to assume that the MC  $P(p)$  curves have the same shape as the  $R(p)$  curves, but are simply shifted to the left, parallel to the  $p$  axis. One then must make an assumption regarding the range of validity of Eq. (2). The assumption that Eq. (2) is valid only over a short range of values of  $p$  demands that we use only the first few data points in our calculations. This procedure we will call method IA. Method IB consists of using all the data points available for the lattice, again under the assumption that  $P(p)$  has the same shape as  $R(p)$ .

An alternative suggested by Fisher<sup>13</sup> is to suppose that all data points to the left of the exact (or series values, if exact values are unknown) value of  $p_c$  are spurious, and to calculate  $\beta$  using the exact value of  $p_c$ . This method will be called method II. Calculations using  $p_c$  as a fitting parameter in minimizing  $\sigma^2$  in Eq. (3) proved to be inconclusive, presumably due to a shortage of the number of data points for larger values of  $p - p_c$ .

The values of  $\beta$  quoted in the following are found by minimizing numerically the squared deviation<sup>14</sup>

$$\sigma^2(\beta) = \sum_{i=1}^N [R(p_i) - (p_i - p_c)^\beta]^2, \quad (3)$$

where  $N$  is the number of data points  $[p_i, R(p_i)]$  used. Errors in values of  $\beta$  so obtained can arise

TABLE I. Values of  $\beta$ . The error estimates are from Eq. (4).

Lattice	Method		
	IA	IB	II
fcc, hcp			
bond problem	$0.23 \pm 0.11$	$0.13 \pm 0.03$	$0.08 \pm 0.01$
Triangular			
bond problem	$0.49 \pm 0.15$	$0.15 \pm 0.03$	$0.07 \pm 0.015$
site problem	$0.24 \pm 0.09$	$0.14 \pm 0.04$	$0.04 \pm 0.01$
Honeycomb			
bond problem	$0.25 \pm 0.07$	$0.15 \pm 0.03$	$0.05 \pm 0.01$
site problem	$0.24 \pm 0.07$	$0.16 \pm 0.04$	$0.04 \pm 0.01$

both from errors estimated for the values of  $R(p_i)^3$  and from the error measured by  $\sigma$  in the least-squares fit. Combining these sources one obtains the estimates

$$\Delta\beta = \max_i \left| \frac{(\sigma^2/N(N-1) + R(p_i)[1-R(p_i)]/M)^{1/2}}{(p_i - p_c)^\beta \ln(p_i - p_c)} \right|, \quad (4)$$

which are the errors quoted in Table I. Here  $M = 100$  for  $d=2$ , and  $M=50$  for  $d=3$ . The quantity  $R(p_i)[1-R(p_i)]$  was replaced by its maximum value 0.25 in all error estimates. While Eq. (4) is an explicit formula for a given method (i.e., set of data points), it is evident that the actual values of  $\beta$  obtained depend strongly upon the method used.

The results of the calculations are shown in Table I and a graph of the results for a sample problem, the honeycomb-lattice bond problem, is shown in Fig. 1. The figure shows graphically the differences in the curves predicted by the three methods. In this example, the lowest five data points were used in method IA, with  $p_c = 0.61$ , the value dictated by the assumptions made for the method. Curve IB results from using all sixteen data points with  $p_c = 0.61$  for this case also. Thus IA is the best fit to the first five points, while IB is the best fit to all the points, for the chosen value of  $p_c$ . On the other hand, curve II was obtained using the exact value  $p_c = 0.65273$ , neglecting the points with  $p < p_c$ . The calculations using  $p_c$  as a fitting parameter included all three methods as special cases. As mentioned above, these calculations proved to be inconclusive in determining the

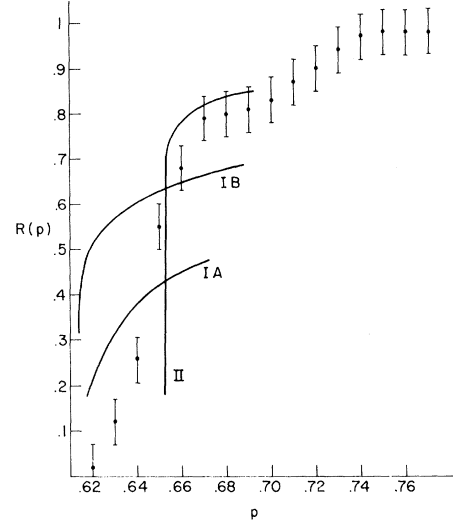


FIG. 1. Data points with error bars and the curves calculated according to the various methods described in the text for the honeycomb-lattice bond problem.

best value of  $p_c$ .

The three methods differ widely in their respective predictions, method IA suggesting that  $\beta = \frac{1}{4}$ ; method IB,  $\beta = 0.15$  (possibly  $\frac{1}{6}$ ); and method II,  $\beta = 0.05$  [possibly  $\beta = 0$ , indicating that  $R(p)$  is a step function] for the two-dimensional lattices. However, each method appears to be internally consistent in predicting the same values for both problems in all lattices, with the exception of the triangular-lattice bond problem, for which  $\beta$  is significantly higher according to the methods IA and II. Hence, with the exception of this case, all the  $R(p)$  curves appear to be of the same shape.<sup>15</sup>

Although the present results suffer from an ambiguity in the actual values of  $\beta$  for the various lattices, one can conclude, at least, that it is reasonable to attempt to apply the usual critical-point analysis techniques to percolation problems. The interesting question of whether or not the triangular-lattice bond problem does indeed have a different  $\beta$  from that of the other two-dimensional lattices remains to be examined more fully by more sophisticated analytical techniques. It is to be hoped that this work will encourage further efforts in the study of the details of critical behavior in percolation processes.

\*Research supported in part by the National Science Foundation through Grant No. GP-8449.

<sup>1</sup>V. A. Vyssotsky, S. B. Gordon, H. L. Frisch, and J. M. Hammersley, Phys. Rev. **123**, 1566 (1961).

<sup>2</sup>H. L. Frisch, E. Sonnenblick, V. A. Vyssotsky, and J. M. Hammersley, Phys. Rev. **124**, 1021 (1961).

<sup>3</sup>H. L. Frisch, J. M. Hammersley, and D. J. A. Welsh, Phys. Rev. **126**, 949 (1962).

<sup>4</sup>S. R. Broadbent and J. M. Hammersley, *Proc. Cambridge Phil. Soc.* **53**, 629 (1957).

<sup>5</sup>Review articles are H. L. Frisch and J. M. Hammersley, *J. Soc. Indust. Appl. Math.* **11**, 894 (1963); M. E. Fisher, *Proceedings of the IBM Scientific Computing Symposium on Combinatorial Problems*, 1964 (IBM Data Processing Division, White Plains, N. Y., 1966), p. 179.

<sup>6</sup>M. E. Fisher and J. W. Essam, *J. Math. Phys.* **2**, 609 (1961).

<sup>7</sup>P. W. Kasteleyn and C. M. Fortuin, *J. Phys. Soc. Japan Suppl.* **26**, 11 (1969).

<sup>8</sup>R. B. Griffiths, *J. Math. Phys.* **8**, 484 (1967).

<sup>9</sup>H. L. Frisch, S. B. Gordon, V. A. Vyssotsky, and J. M. Hammersley, *Bell System Tech. J.* **41**, 909 (1962).

<sup>10</sup>M. E. Fisher in Ref. 5.

<sup>11</sup>M. F. Sykes and J. W. Essam, *Phys. Rev. Letters* **10**, 3 (1963); *J. Math. Phys.* **5**, 1117 (1964).

<sup>12</sup>M. F. Sykes and J. W. Essam, *Phys. Rev.* **133**, A310 (1964).

<sup>13</sup>M. E. Fisher, at the Statistical Mechanics Meeting of the Belfer Graduate School of Science, December, 1969 (unpublished).

<sup>14</sup>The computer work was carried out using the Univac 1108 computer at the Computer Center of the State University of New York at Albany.

<sup>15</sup>Which fact may be taken as an indication that fluctuations in the data due to the proximity of the critical point are insignificant.

## Effects of Hydrostatic Pressure on the Magnetic Ordering of Heavy Rare Earths\*

G. S. Fleming<sup>†</sup> and S. H. Liu

*Institute for Atomic Research and Department of Physics, Iowa State University, Ames, Iowa 50010*

(Received 9 February 1970)

The effects of hydrostatic pressure on the magnetic ordering of heavy rare earths are studied through the pressure shift of the electronic energy bands and the effects of this pressure shift on the indirect exchange. It is shown that the change in the ordering temperature of Gd, Tb, and Dy and the variation of the helical turn angle of Tb can be explained in this manner.

Many experiments have been performed to study the effects of hydrostatic pressure on the magnetic ordering of heavy rare earths.<sup>1-6</sup> Below a certain critical pressure where a crystallographic transition takes place, the magnetic ordering temperature of Gd, Tb, Dy, and Ho was found to decrease linearly with pressure by the order  $-1$  K/kbar. The type of initial magnetic ordering is unchanged by pressure, i.e., just below the ordering temperature Gd is ferromagnetic while Tb, Dy, and Ho are antiferromagnetic.<sup>4,6</sup> However, neutron diffraction experiments have revealed a reduction of helical turn angle in Tb and Ho when pressure is applied.<sup>6</sup> The purpose of our work is to explain these results from the point of view that the magnetic ordering of these metals is to a large extent determined by their electronic energy bands and Fermi-surface geometry.<sup>7-9</sup> It will be shown that this approach does give a quantitative understanding of the observed effects.

The program of our study proceeds by first calculating the electronic energy bands of the metal under study, then computing the generalized susceptibility function  $\chi(\vec{q})$  for a  $\vec{q}$  vector along the  $c$  axis, and finally correlating the location and the size of the peak of  $\chi(\vec{q})$  with the magnetic ordering properties. This is done for Gd, Tb, and Dy under

0 and 20 kbar of pressure. The pressure effects are deduced from the shift of the  $\chi(\vec{q})$  curve. In the following paragraph we explain briefly these calculations.

We used the relativistic augmented-plane-wave (RAPW) method for the energy band calculation,<sup>10</sup> the details of which are given in Ref. 7. The crystal potential was approximated by a muffin-tin potential constructed from a superposition of atomic potentials including the full Slater exchange. The lattice parameters under pressure were deduced from the elastic constants of Gd,<sup>11</sup> Tb,<sup>12</sup> and Dy.<sup>13,14</sup> Their actual values are listed in Table I. The radius of the augmented-plane-wave (APW) sphere was chosen as 3.32 a.u. for Gd and as 3.16 a.u. for Tb and Dy. The same APW sphere radius was used for both the zero-pressure and the 20-kbar calculations. We selected a set of 32 plane waves as the basis functions so that the band calculation was convergent to within 0.002 Ry. Energy eigenvalues were calculated over a mesh of 147 points in 1/24th zone. The spline interpolation method was used to interpolate the bands over a mesh of 450 000 points in the full zone. The susceptibility calculation was fully described in Ref. 9. With the interpolated bands, we calculated  $\chi(\vec{q})$  for  $\vec{q}$  along  $\Gamma\text{A}\Gamma$  in the double zone scheme over a